Journal Pre-proofs

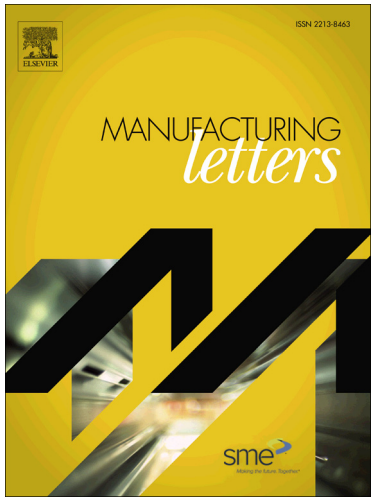

Material characterisation using electronic imaging for Electron Beam Melting process monitoring

Hay Wong, Rebecca Garrard, Kate Black, Peter Fox, Chris Sutcliffe

PII: S2213-8463(19)30143-9
DOI: https://doi.org/10.1016/j.mfglet.2019.12.005
Reference: MFGLET 220

To appear in: *Manufacturing Letters*

Received Date: 9 October 2019
Revised Date: 3 December 2019
Accepted Date: 14 December 2019

Please cite this article as: H. Wong, R. Garrard, K. Black, P. Fox, C. Sutcliffe, Material characterisation using electronic imaging for Electron Beam Melting process monitoring, *Manufacturing Letters* (2019), doi: https://doi.org/10.1016/j.mfglet.2019.12.005

Material characterisation using electronic imaging for Electron Beam Melting process monitoring

Authors: Hay Wong[a], Rebecca Garrard[a], Kate Black[a], Peter Fox[a], Chris Sutcliffe[a]

[a]School of Engineering, University of Liverpool, The Quadrangle, Brownlow Hill, United Kingdom L69 3GH

Corresponding author's email: Hay Wong – hay.wong@liv.ac.uk

Keywords: Electron Beam Melting; Material Characterisation; Quality Control; In-Situ; Additive Manufacturing

Abstract

In-situ process monitoring in Electron Beam Melting (EBM) is critical in certifying build quality, by identifying contamination from the feedstock and condensate spallation from within the build area. The chamber condition in an EBM machine is different from a typical electron microscope. Therefore this study explores in-situ EBM material characterisation with a custom electronic imaging prototype. Typical contamination elements found in a popular EBM material (Ti-6Al-4V) were electronically imaged at room temperature. Material contrast is observed in the electronic images generated by the prototype. This trial is thought to serve as a baseline study for future EBM monitoring system development.

1. Introduction

1.1 Electron Beam Melting monitoring

Electron Beam Melting (EBM) is a metal Additive Manufacturing (AM) technique which uses an electron beam to process metallic powder in a layer-wise fashion [1]. The EBM process offers various benefits, including: a reduction in thermal residual stress within components [2], and a high level of design freedom [3,4]. Nevertheless, the EBM process is prone to quality issues such as in-layer porosity [5] and layer-delamination [6]. Current monitoring techniques being investigated include optical cameras [7], thermal cameras [8–10], and electronic imaging systems [11, 12]. Arnold et al [12, 13] developed an electronic imaging system for a modified Arcam S12 EBM machine, and Wong et al [11, 14-16]

developed a custom electronic imaging prototype for an Arcam A1 EBM machine. Despite the research efforts made by Arnold et al and Wong et al, no information is available regarding the material characterisation ability of such electronic imaging systems. The ability to differentiate materials in-situ could enable Quality Control (QC) over issues such as, powder feedstock contamination and metallisation.

1.2 Research gap: in-situ EBM material characterisation with electronic imaging

With regard to powder contamination, firstly, an AM machine in industry often needs to handle multiple feedstock materials to maintain shop-floor efficiency [17]. For example, tungsten [18] and Ti-6Al-4V [19] are two popular AM materials in the aerospace industry. Tungsten is used as balancing weights in rotor blades due to its high density [20], whilst Ti-6Al-4V is used for fracture-critical parts including airframe and compressor blades due to its suitable strength-toughness combinations [21]. A prior study on cross-contamination between tungsten and Ti-6Al-4V powder shows that contamination affects mechanical strength of components [22]. Secondly, the production of AM powder is another contamination source. It has been reported that the tungsten electrode used in typical powder production equipment wears out and leads to tungsten particles mingled in the powder batch [22].

Regarding metallisation, high vapour pressure and low melting point elements in the powder feedstock vaporise and condense onto the interior surface of the EBM machine chamber during material processing [23]. These condensates forms metallised layers during the EBM build cycle, and at times crack and fall off onto the processing area [23]. Metallisation flakes on the processing area affects material processing and the integrity of the components being made [24], whilst metallisation condensing onto optical camera lens / protective Kapton® film affects the quality of in-situ process inspection [8, 25]. Metallisation has been reported to have different compositions when compared to its powder feedstock. Metallisation from a Ti-6Al-4V build has for instance been reported to be rich in $TiAl_3$ [23].

In-situ material characterisation via electronic imaging has the potential to detect powder contamination and metallisation contamination of the bed. A typical Scanning Electron Microscope (SEM) can be used to study and characterise materials in specimens [26]. Common techniques include, Backscattered Electrons (BSE) imaging, X-ray analysis, and electron channelling patterns [26]. These techniques all require the use of sophisticated sensors, which are too delicate to operate inside an EBM machine for monitoring purposes.

When compared to a typical SEM, a standard EBM machine operates at: (1) higher processing area temperature, i.e. up to 700 ºC [27, 28], (2) higher electron gun accelerating voltage, i.e. 60 kV [29, 30], (3) lower chamber pressure level, i.e. 2 x 10^{-3} mbar [29, 31], (4) greater working distance, i.e. 400 mm [27, 32], and (5) larger imaging area, i.e. 200 mm x 200 mm [29, 33]. These differences affect the following aspects in feedback electron signal collection during imaging: (1) electron yield is sensitive to the electron beam accelerating voltage, (2) the increase in imaging area amplifies the surface-tilt variation in the signal, (3) signal noise might be induced by thermionic emission due to high temperature, and electron-gas amplification due to low vacuum in the machine chamber. This study aims to investigate in-situ EBM material characterisation with electronic imaging. As a precursor to more elaborated studies in the future, the main goal of this pilot study is to explore if the imaging prototype developed by Wong et al [11] is capable of discerning different materials when conducting electronic imaging in an Arcam A1 EBM machine at room temperature.

2. Materials and Methods

Fig. 1 describes an electronic imaging prototype [11, 13] used in this study. The prototype consists of a feedback electron sensor (modified Arcam heat-shield frame and plates), a data logger (Arduino DUE microcontroller break-out board), signal amplifier and electronic image generation software. The prototype is designed to interface with the Arcam A1 EBM machine to generate digital electronic images from the feedback electrons collected, i.e. Secondary Electrons (SE) and BSE. These feedback electrons originate from the interactions between the machine electron beam and the area being imaged.

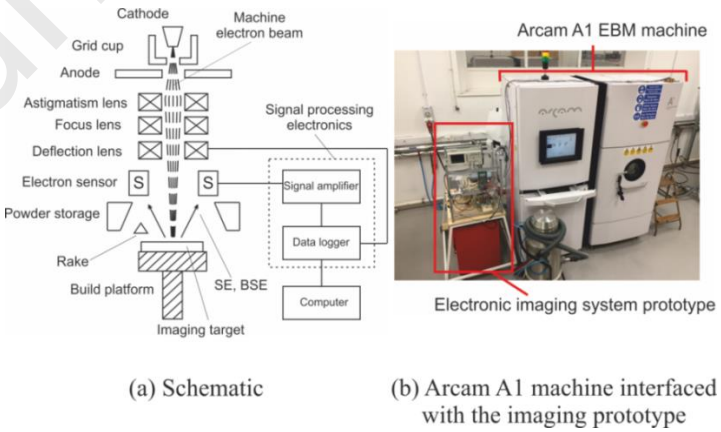

Fig. 1 Custom imaging prototype interfaced with a commercial EBM machine [11, 14]

Fig. 2 illustrates the imaging target plate, herein referred to as the "plate", and the inserts involved in this study. The 210 mm x 210 mm x 5 mm plate was machined from a 316L stainless steel plate (The Metal Store, UK) with a waterjet cutting machine (OMAX, USA). Nine location markers and 27 pockets, as shown in Fig. 2 (a), were machined across the plate with a computer numerical control machine (HAAS, USA). Three materials were chosen to be investigated in this pilot study: silicon (to represent aluminium as: 1. They have similar atomic numbers, 2. Silicon has a higher melting temperature), Ti-6Al-4V, and tungsten, due to their presence in EBM powder feedstock contamination and metallisation, as described in Section 1.2. Figs. 2 (b) and (c) show the inserts in position and the critical dimensions in the setup. The 5 mm x 5 mm x 0.3 mm silicon inserts were cleaved from a typical silicon wafer (PI-KEM, UK); the ϕ10 mm x 5 mm Ti-6Al-4V inserts were machined from a Ti-6Al-4V rod (GoodFellow, UK) with a conventional lathe; and the ϕ10 mm x 5 mm tungsten inserts were machined from a tungsten rod (GoodFellow, UK) with a wire electrical discharged machine (ONA, Spain). Table 1 details the experimental configurations of the imaging prototype and the Arcam A1 EBM machine used in this in-situ material characterisation pilot study.

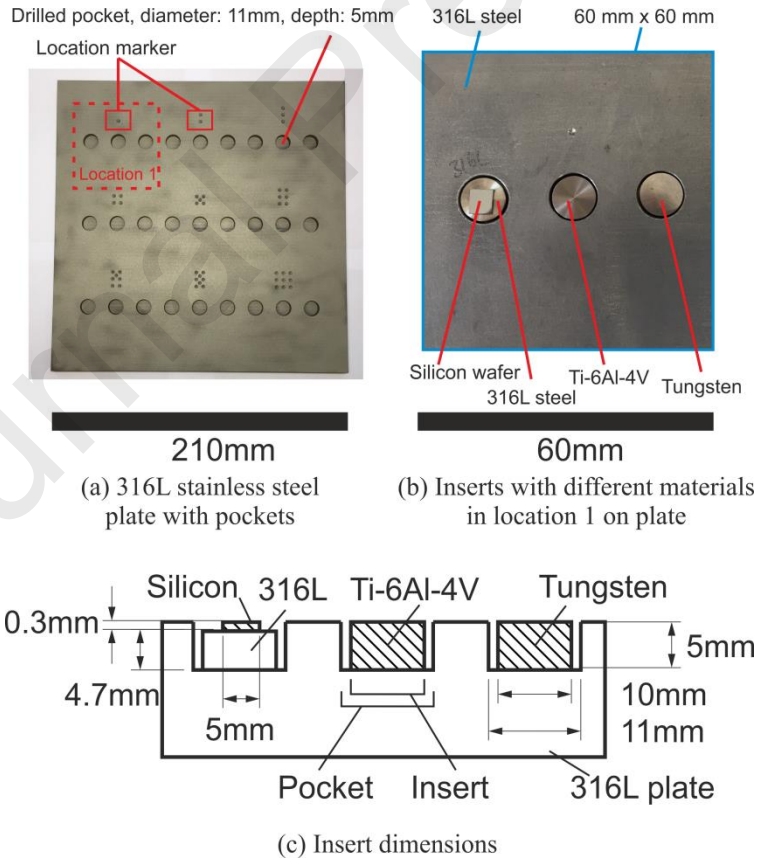

Fig. 2 Imaging experimental setup

Table 1 Experimental configuration

Parameter	Value
Imaging Prototype	
Imaging area	60 mm x 60 mm
Imaging location	1
Image size	1800 x 1800 pixels
Image bit depth	8-bit, 256 levels
Data logger sampling frequency	118.8 kHz
Arcam A1 EBM Machine	
Beam accelerating voltage	60 kV
Beam current	1 mA
Beam speed	3960 mms^{-1}
Beam focus offset	0 mA

3. Results

Fig. 3 (a) is a typical raw electronic image generated from one of the off-centre locations (an extreme case to showcase independence from signal shadowing effect), i.e. “location 1”, of the plate with three different inserts in place. The pixel row indicated by the dotted line in the image was extracted for data analysis. Fig. 3(b) shows the pixel value profile of the extracted pixel row. As the image is in 8-bit greyscale, a pixel value of “0” represents the colour black, whilst a value of “255” represents the colour white. The pixel value is directly proportional to the signal strength of the feedback electrons sampled. The pixel value profile shown in Fig. 3 (b) illustrates that the electronic image generated by the imaging prototype is material sensitive. Silicon, Ti-6Al-4V, 316L steel, and tungsten all have different pixel values. Moreover, sharp troughs are observed between different material sections in the profile plot.

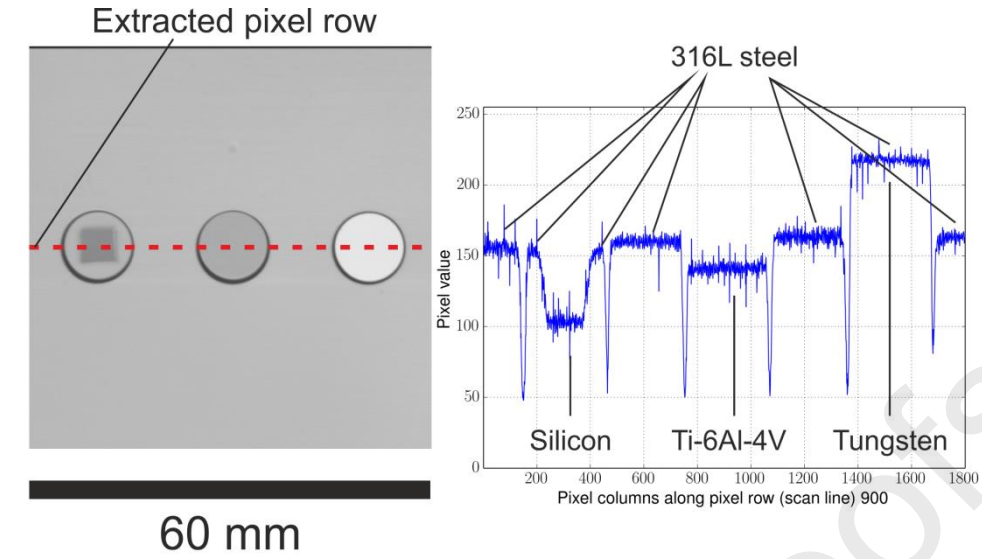

(a) Electronic image of location 1. Materials (left to right): silicon, Ti-6Al-4V, and Tungsten

(b) Image pixel value profile of the extracted pixel row

Fig. 3 Electronic image demonstrating material contrast

4. Discussion

Difference in image contrast can be seen when comparing Fig. 2 (b), an optical image, with Fig. 3 (a), an electronic image. Material contrast stands out in the electron image. The atomic numbers of the materials investigated in this study are as follows: silicon (14) – representing aluminium-rich aluminides (e.g. $TiAl_3$), titanium (22) - representing Ti-6Al-4V, iron (26) - representing 316L steel, and tungsten (74). It can be seen from Fig. 3 (b) that the pixel value (feedback electron signal strength) is dependent of the atomic number of the materials being imaged.

Sharp troughs are observed in Fig. 3 (b) as the inserts involved in this study all have a diameter of 10 mm, whilst the pockets on the plate have a diameter of 11 mm. There are gaps between the pockets and the inserts. During imaging, the feedback electron signal strength is at its minimum at these gaps, as the SE and BSE emitted are more likely to be re-absorbed by their surroundings and therefore could not reach the sensor.

Within each material section in Fig. 3 (b), shot noise presents itself as spikes. Shot noise comes from the current fluctuation due to the discrete transfer of charges [34]. The electron beam has a statistical distribution when hitting the specimen during a given image pixel time. As SE and BSE are generated from the interaction between the primary electrons and the

specimen, they too show similar distribution, which manifests itself as shot noise in the feedback electron signal [34].

5. Conclusions

This study investigates in-situ material characterisation for the EBM process. Electronic imaging was carried out with a custom imaging prototype operating inside a commercial EBM machine at room temperature. Despite the differences in the chamber environment between a typical SEM and a standard EBM machine, the raw electronic images generated in this study display material contrast between the materials investigated (silicon, Ti-6Al-4V, 316L stainless steel, and tungsten). This material characterisation capability could open up new opportunities in custom-built EBM monitoring systems for QC purposes. In order to realise this potential, the authors have planned further studies to investigate other factors which might obscure the image material contrast. These include: high in-situ EBM temperature (>650ºC), resolving power of the EBM electron beam, packing density of the powder feedstock, location-dependence in feedback electrons sampling, and the influence of electron-gas ionisation induced signal noise. This pilot trial serves as a precursor, setting a baseline and laying the foundation for further investigations.

Acknowledgements

The Author(s) declare(s) that there is no conflict of interest. The EBM machine was purchased, in part from a grant received for the EPSRC Centre for Innovative Manufacturing in Additive Manufacturing. EP/I033335/2.

7. References

1. I. Gibson, D.W. Rosen, B Stucker (2010) Additive Manufacturing Technologies. Springer, New York, pp. 126-128

2. G. Baudana, S. Biamino, D. Ugues, M. Lombardi, P. Fino, M. Pavese, C. Badini, (2016) Titanium Aluminides for Aerospace and Automotive Applications Processed by Electron Beam Melting: Contribution of Politecnico di Torino, Metal Powder Report, Volume 71, Issue 3, 2016, Pages 193-199, ISSN 0026-0657, http://dx.doi.org/10.1016/j.mprp.2016.02.058.

3. O.L.A Harrysson, O. Cansizoglu, D.J. Marcellin-Little, D.R Cormier, H.A West (2008) Direct Metal Fabrication of Titanium Implants with Tailored Materials and Mechanical Properties using Electron Beam Melting Technology, Materials Science and Engineering: C, Volume 28, Issue 3, 2008, Pages 366-373, ISSN 0928-4931, http://dx.doi.org/10.1016/j.msec.2007.04.022.

4. G. Baudana, S. Biamino, D. Ugues, M. Lombardi, P. Fino, M. Pavese, C. Badini, Titanium aluminides for aerospace and automotive applications processed by electron beam melting: contribution of Politecnico di Torino, metal powder report, Volume 71, Issue 3, 2016, Pages 193-199, ISSN 0026-0657 (2016) http://dx.doi.org/10.1016/j.mprp.2016.02.058.
5. P. Stravroulakis R.K. Leach A.T. Clare S.K. Everton, M. Hirscha (2016) Review of in-situ process monitoring and in-situ metrology for metal additive manufacturing. Materials and Design, 95:431–445, 2016. DOI: http://dx.doi.org/10.1016/j.matdes.2016.
6. W. J. Sames (2015) Additive Manufacturing of Inconel 718 Using Electron Beam Melting: Processing, Post-Processing, & Mechanical Properties. PhD thesis, Texas A&M University, Nuclear Engineering
7. Scharowsky T, Bauereiß A, Singer RF, Körner C (2012) Observation and numerical simulation of melt pool dynamic and beam powder interaction during selective electron beam melting, Proceedings from the Solid Freeform Fabrication Symposium, Austin, pp 815–8205.
8. Raplee J, Plotkowski A, Kirka MM, Dinwiddie R, Okello A, Dehoff RR, Babu SS (2017) Thermographic microstructure monitoring in electron beam additive manufacturing, Scientific Reports 7, Article Number: 43554. doi:10.1038/srep43554
9. Price S, Lydon J, Cooper K, Chao K (2013) Experimental temperature analysis of powder-based electron beam additive manufacturing, Proceedings from the Solid Freeform Fabrication Symposium, pp. 162-173
10. Cordero PM, Mireles J, Ridwan S, Wicker RB (2017) Evaluation of monitoring methods for electron beam melting powder bed fusion Additive Manufacturing Technology, Progress in Additive Manufacturing, June 2017, Volume 2, Issue 1-2, pp 1-10, https://doi.org/10.1007/s40964-016-0015-6
11. Wong H, Neary D, Shahzad S, Jones E, Fox P, Sutcliffe C (2019) Pilot investigation of feedback electronic image generation in electron beam melting and its potential for

in-process monitoring, Journal of Materials Processing Tech., 266, 502-517, DOI: 10.1016/j.jmatprotec.2018.10.016

12. Arnold C, Pobel C, Osmanlic F, Körner C (2018) Layerwise monitoring of electron beam melting via backscatter electron detection, Rapid Prototyping Journal 24/8 (2018) 1401–1406. DOI: 10.1108/RPJ-02-2018-0034
13. Robel CR, Arnold C, Osmanlic F, Fu Zongwen, Körner (2019) Immediate development of processing windows for selective electron beam melting using layerwise monitoring via backscattered electron detection, Materials Letters, Vol 249, pp. 70-72, DOI: 10.1016/j.matlet.2019.03.048
14. Wong H, Neary D, Jones E, Fox P, Sutcliffe C (2019) Pilot feedback electronic imaging at elevated temperatures and its potential for in-process electron beam melting monitoring, Additive Manufacturing, 27, 185-198, DOI: 10.1016/j.addma.2019.02.022
15. Wong H, Neary D, Jones E, Fox P, Sutcliffe C (2018) Pilot capability evaluation of a feedback electronic imaging system prototype for in-process monitoring in electron beam additive manufacturing, Springer International Journal of Advanced Manufacturing Technology, DOI: 10.1007/s00170-018-2702-6
16. Wong H, Neary D, Jones E, Fox P, Sutcliffe C (2019) Benchmarking spatial resolution in electronic imaging for potential in-situ electron beam melting monitoring, Additive Manufacturing, 29, 100829, DOI: 10.1016/j.addma.2019.100829
17. D' Angelo G, Resebo E, Pedersen DB, Harrysson O, Challenges and quality implications of feedstock cross-contamination of metal powders: an industrial perspective (2017)AMEXCI AB study, http://amexci.com/wp-content/uploads/2019/07/5191.pdf
18. Wang DZ, Yu CF, Zhou X, Ma J, Liu W, Shen ZJ (2017) Dense pure tungsten fabricated by selective laser melting, Appl. Sci. 2017, Vol 7 (issue 4), 430, DOI:10.3390/app7040430
19. Loureiro AJR, Veiga C, Davim JP (2012) Properties and applications of titanium alloys: A brief review. Rev. Adv. Mater. Sci, 32, pp. 133–148
20. A. Arora, V.G. Rao (2016) Tungsten heavy alloy for defence applications, Materials Technology, 19:4, 210-215, DOI: 10.1080/10667857.2004.11753087
21. I. Inagaki, T. Takechi, Y. Shirai, N. Ariyasu (2014) Application and features of titanium for the aerospace industry, Nippon steel & Sumitomo metal technical report No. 106

22. Lütjering, G.; Williams, J.C. Titanium, Engineering Materials and Processes; Springer Science & Business Media: Berlin, Germany, 2007; Chapter 3.
23. Nandwana P, Peter WH, Dehoff RR, Lowe LE, Kirka MM, Medina F, Babu SS (2015) Recyclability study on Inconel 718 and Ti-6Al-4V powders for use in Electron Beam Melting, Metallurgical and Materials Transactions B, Vol 47B, pp. 754 – 762, DOI: 10.1007/s11663-015-0477-9
24. Tan XP, Kok Y, Tor SB, Chua CK (2014) Application of Electron Beam Melting (EBM) in additive manufacturing of an impeller, Proc. of the Intl. Conf. on Progress in Additive Manufacturing, DOI:10.3850/978-981-09-0446-3 076
25. Dinwiddie RB, Dehoff RR, Lloyd PD, Lowe LE, Ulrich JB (2013) Thermographic in-situ process monitoring of the Electron Beam Melting technology used in additive manufacturing, Proc. of SPIE Vol. 8705, DOI: 10.1117/12.2018412
26. Beauvais J, Drouin D, Gauvin R (1997) SEM techniques for materials characterization, Proc. of SPIE Vol. 10291 102910B-1, DOI: 10.1117/12.279839
27. Luft J, Weißgarber T, Kieback B, Kirchner A, Klöden B. Process window for electron beam melting of Ti-6Al-4V. In Euro PM2014 – AM: Technologies Manuscript (2014)
28. Holmes, JL, Bachus KN, Bloebaum RD (2000) Thermal effects of the electron beam and implications of surface damage in the analysis of bone tissue, SCANNING VOL. 22, 243–248, DOI: 10.1002/sca.4950220403
29. Gong X, Anderson T, Chou K (2014) Review on powder-based electron beam additive manufacturing technology, Manufacturing Rev. 2014, 1, 2, DOI: 10.1051/mfreview/2014001
30. L. Reimer. Scanning electron microscopy: Physics of image formation and microanalysis, pages 13–19. Springer (1998) ISBN: 3-540-63976-4
31. JEOL. SEM scanning electron microscope A to Z: basic knowledge for using the SEM. Pages: 23-26. https://www.jeol.co.jp/en/applications/pdf/sm/sem_atoz_all.pdf
32. A. Gunasekaran. Scanning electron microscopy. course material, LA SIGMA Microscopy workshop, the LONI Institute, https://www.institute.loni.org/lasigma/document_files/workshopdocuments/SEMnotes.pdf
33. I.M.Watt. The principle and practice of electron microscopy, page 162. Cambridge University Press, 1997. ISBN: 9780521435918, http://ebooks.cambridge.org/
34. L. Reimer (1998) Scanning Electron Microscopy: Physics of Image Formation and Microanalysis, Springer, pp. 165 – 166